Clim. Past, 7, 1459–1469, 2011
www.clim-past.net/7/1459/2011/
doi:10.5194/cp-7-1459-2011

Climate of the Past

Reconstruction of a continuous high-resolution CO_2 record over the past 20 million years

R. S. W. van de Wal[1], B. de Boer[1], L. J. Lourens[2], P. Köhler[3], and R. Bintanja[4]

[1]Institute for Marine and Atmospheric research Utrecht, Utrecht University, Princetonplein 5, 3584 CC Utrecht, The Netherlands
[2]Department of Earth Sciences, Faculty of Geosciences, Utrecht University, Budapestlaan 4, 3584 CD Utrecht, The Netherlands
[3]Alfred Wegener Institute for Polar and Marine Research, P.O. Box 120161, 27515 Bremerhaven, Germany
[4]Royal Netherlands Meteorological Institute (KNMI), Wilhelminalaan 10, 3732 GK De Bilt, The Netherlands

Received: 29 December 2010 – Published in Clim. Past Discuss.: 2 February 2011
Revised: 26 October 2011 – Accepted: 14 November 2011 – Published: 21 December 2011

Abstract. The gradual cooling of the climate during the Cenozoic has generally been attributed to a decrease in CO_2 concentration in the atmosphere. The lack of transient climate models and, in particular, the lack of high-resolution proxy records of CO_2, beyond the ice-core record prohibit, however, a full understanding of, for example, the inception of the Northern Hemisphere glaciation and mid-Pleistocene transition. Here we elaborate on an inverse modelling technique to reconstruct a continuous CO_2 series over the past 20 million year (Myr), by decomposing the global deep-sea benthic $\delta^{18}O$ record into a mutually consistent temperature and sea level record, using a set of 1-D models of the major Northern and Southern Hemisphere ice sheets. We subsequently compared the modelled temperature record with ice core and proxy-derived CO_2 data to create a continuous CO_2 reconstruction over the past 20 Myr. Results show a gradual decline from 450 ppmv around 15 Myr ago to 225 ppmv for mean conditions of the glacial-interglacial cycles of the last 1 Myr, coinciding with a gradual cooling of the global surface temperature of 10 K. Between 13 to 3 Myr ago there is no long-term sea level variation caused by ice-volume changes. We find no evidence of change in the long-term relation between temperature change and CO_2, other than the effect following the saturation of the absorption bands for CO_2. The reconstructed CO_2 record shows that the Northern Hemisphere glaciation starts once the long-term average CO_2 concentration drops below 265 ppmv after a period of strong decrease in CO_2. Finally, only a small long-term decline of 23 ppmv is found during the mid-Pleistocene transition, constraining theories on this major transition in the climate system. The approach is not accurate enough to revise current ideas about climate sensitivity.

Correspondence to: R. S. W. van de Wal (r.s.w.vandewal@uu.nl)

1 Introduction

The overall climate cooling reconstructed for the past 20 Myr has generally been attributed to a change in CO_2 concentration in the atmosphere (Zachos et al., 2008; Ruddiman, 2003), although the amount of CO_2 decreases and the amplitude of subsequent cooling are discussed widely (Jansen et al., 2007). Since data and modelling studies covering this time period are poorly integrated, our understanding of the inception of ice ages in the Northern Hemisphere (NH) (Raymo 1994), as well as the mechanisms causing the transition from 41 000-yr to 100 000-yr dominated climate cycles (Tziperman and Gildor, 2003; Clark et al., 2006; Huybers, 2007; Bintanja and Van de Wal, 2008), that occurred without apparent changes in the insolation forcing (Hays et al., 1976; Imbrie and Imbrie, 1980) is still incomplete. Current difficulties in assessing the role of CO_2 on the long timescales are the lack of reliable CO_2 data from the pre ice-core record (Ruddiman, 2010), and the limited data of sea level (Miller et al., 2005; Müller et al., 2008) and temperature (De Boer et al., 2010). Our current knowledge of long-term climate variability builds on the Milankovitch theory of solar-insolation variability (Milankovitch 1941), including scenarios that rely on highly parameterized nonlinear response mechanisms to the insolation forcing. Recent developments in the interpretation of marine $\delta^{18}O$ records and new CO_2 proxies allow

us to reassess this understanding and to present a global overview of temperature, sea level and CO_2 changes over time.

We build on a model set-up that aims to integrate the main climate variables, temperature and sea level, of the glacial-interglacial variability over the past 20 Myr (Bintanja et al., 2005a, b; Bintanja and van de Wal, 2008; De Boer et al., 2010, 2011) to reconstruct changes in past CO_2 concentrations. The model takes advantage of the mass conservation of δ^{18}O on a global scale, while an inverse routine guarantees that changes in ocean δ^{18}O caused by both land ice sheet growth (sea-level change) and deep ocean temperature change are in agreement with marine benthic δ^{18}O reconstructions. Output of the model is ice volume and the change in NH air temperature (ΔT_{NH}) relative to the present day, calculated from the deep ocean temperature, which gives an estimate of the air temperatures at sea level in areas where the NH ice sheets developed (40°–80° N). Here we will use the ΔT_{NH} derived by De Boer et al. (2010) to reconstruct a continuous CO_2 record over the past 20 Myr.

For this purpose, we compared the T_{NH} record, with existing proxies for CO_2, first for the past 800 000 yr using primarily ice-core CO_2 data (Petit et al., 1999; Siegenthaler et al., 2005; Lüthi et al., 2008), and secondly with geochemical and stomata-derived CO_2 proxy data for the older time interval (Tripati et al., 2009; Kürschner et al., 1996, 2008; Retallack 2009; Pearson and Palmer, 2000; Hönisch et al., 2009; Pagani et al., 2005, 2009; Seki et al., 2010). Through this comparison, a regression coefficient between temperature and CO_2 could be determined that allowed us to reconstruct a global mutually self-consistent and continuous overview of temperature, sea level and CO_2 over the past 20 Myr. Eventually the paper is concluded by a discussion on climate sensitivity following from our results.

2 Inverse δ^{18}O modelling approach

The inverse modelling approach enables the deep-sea benthic δ^{18}O record to be decomposed in a temperature and ice-volume component, using an ice-sheet model. Key processes in the ice-sheet model are a variable isotopic sensitivity and isotopic lapse rate, the mass balance height feedback, the mass balance albedo feedback and the adjustment of the underlying bedrock. In the early stages, the applied model was forced with sea-level reconstructions over the past 120 000 yr (Bintanja et al., 2005a). Through the inverse routine, temperature was adjusted so that modelled ice volume matched the observations. This constraint ensured that sea level and temperature are mutually consistent. In addition, it allowed a quantification of model errors, and errors arising from the uncertainty in the sea-level observations or reconstructions. Results have been compared favourably with sea-level (Rohling et al., 2009; Lambeck and Chapell, 2001) and temperature data (Lear, 2000). The paper by Bintanja et al. (2005a) yielded a T_{NH} reconstruction, which is highly coherent with the classical Vostok temperature record (Petit et al., 1999). Nevertheless, an obvious limitation of this work was that global sea-level observations are limited to the last 0.5 Myr.

In subsequent studies, we, therefore, started to incorporate the marine benthic δ^{18}O record as forcing (e.g. Bintanja et al., 2005b). This was achieved by taking advantage of mass conservation of δ^{18}O on the global scale. First, it was applied to calculate temperature and sea level over the past million years (Bintanja et al., 2005b) and later to explore the mechanisms of the Mid-Pleistocene Transition (Bintanja and Van de Wal, 2008), both focusing on the climate in the NH, as only the Eurasian and North American ice sheet complexes were modelled explicitly. Their temperature reconstruction was compared to alkenone-derived equatorial temperatures (Lawrence et al., 2006) for the last 3 Myr, indicating similar strength for most of the glacials. In order to use the benthic δ^{18}O record as forcing, a simple parameterization was used to separate deep-water temperature from ice-volume changes, based on a linear relation between deep-water temperature and δ^{18}O (Duplessy et al., 2002), and an idealised climate model (Bintanja and Oerlemans, 1996) relating changes in deep-ocean temperature to atmospheric temperature changes (see Bintanja et al., 2005b, 2008 for details).

The last step in the model sequence until now is the explicit inclusion of ice sheets in the Southern Hemisphere (SH), allowing a longer time span to be covered, since for warmer conditions ice-volume changes are dominated by changes in the SH (De Boer et al., 2010). This has been done at the expense of the complexity of the ice-sheet models used. Hence, five 1-D ice sheets, rather than the two 3-D ice-sheet models used previously (Bintanja et al., 2005b; Bintanja and Van de Wal, 2008) were used to reconstruct temperature and sea level over 20 Myr (De Boer at al., 2010). The five 1-D ice-sheet models simulate ice flow over a cone shaped continent. (De Boer et al., 2010). They represent glaciation in Eurasia, North America, Greenland and East and West Antarctica, further abbreviated to NAIS, EAS, GrIS, EAIS, WAIS, respectively, where each has a different geometry, mass balance forcing and isotopic content. Differences between NH and SH temperatures are constant in time and calibrated to match a strong ice volume increase in Antarctica at the Eocene-Oligocene transition (De Boer et al., 2010).

Results of these late Cenozoic runs are compared to sea level by De Boer et al. (2010) with sea level estimates by Miller et al. (2005) and Müller et al. (2008), suggesting considerable differences between 10 and 35 Myr ago. Over the past 10 Myr similarities are high, as the Miller record is derived from the δ^{18}O by scaling. In terms of change in seawater isotope per m sea level change (δw) our results are in good agreement to commonly used values in the literature (De Boer et al., 2011). However, it should be noted that

our modelling approach allows for temporal variations in δw, which is usually not the case. Results of the deep water temperature change since the Miocene by De Boer et al. (2011) are comparable to the results by Lear et al. (2000) based on the Mg/Ca proxy if we use the paleo temperature equation from Shackleton (1974) with a δw present-day value of -0.28 per mille (VPDB). Data by Lear et al. (2010) indicate, however, considerably higher values for the Middle Miocene.

In this model, ΔT_{NH}, determines (1) the growth and retreat of the NAIS, EAS and GrIS, (2) changes in deep-water temperature from which it has been derived, and (3) the SH air temperatures which determine the growth and retreat of the EAIS and WAIS. Hence, besides a simple parameterization to relate deep-water temperature to atmospheric temperature (Bintanja et al., 2005b), we included a constant value to set the temperature difference between the NH and SH. Both parameterizations contribute to the uncertainty of the model as will be explained later. The conceptual approach used here was developed for orbital timescales. Thus, the antiphase dynamics of temperature in the northern and southern high latitudes as observed for the bipolar seesaw (e.g. Barker et al., 2009) is not embedded here, neither are Dansgaard/Oeschger events resolved. Far more detailed models are requested to address these temporal patterns, but the lack of high temporal resolution is not believed to affect the general temporal trends of the orbital timescales addressed here.

In the ice-sheet model, isotopic content and ice volume are calculated with a time step of 1 month and are implemented every 100 yr in the ocean isotope module. Every 100 yr, the modelled benthic isotope is evaluated and forwarded to calculate the temperature anomaly for the next time step (Bintanja et al., 2005b). As forcing we use the stacked benthic δ^{18}O record of Zachos et al. (2008), which is smoothed and interpolated to obtain a continuous record with a resolution of 100 yr. This implies that the timescale of the reconstruction is implicitly determined by the benthic record. The methodology ensures that the phasing between temperature and sea level is consistent with respect to the benthic δ^{18}O data. Further details and a more thorough model description are presented by De Boer et al. (2010).

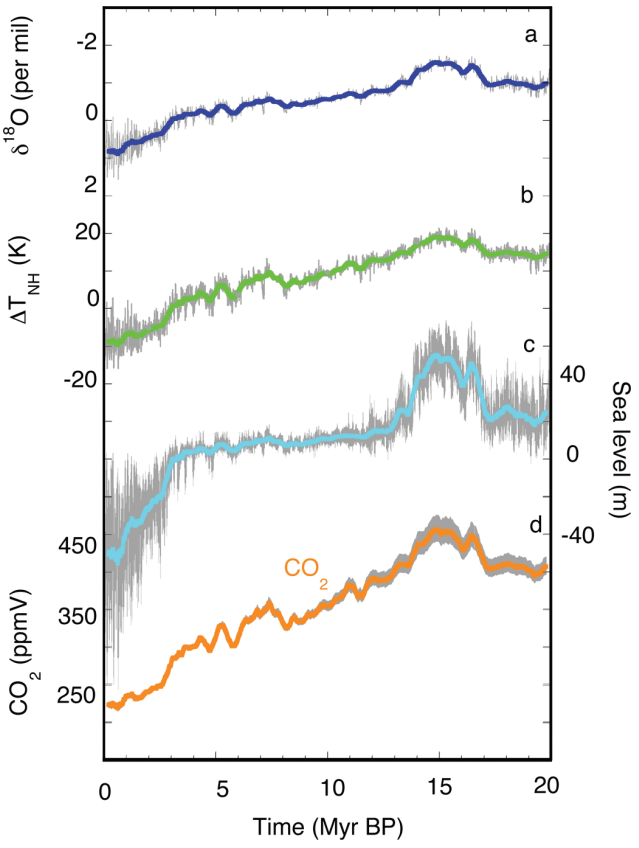

Fig. 1. Records of key climate variables over the last 20 Myr. Forcing of the model are changes in the stacked benthic δ^{18}O record with respect to preindustrial times (a, dark blue, Zachos et al., 2008). Output is a consistent record for the Northern Hemisphere temperature change with respect to pre-industrial conditions (b, green) and sea level (c, light blue). The reconstructed CO_2 record (d, orange) is obtained by inverting the relation between NH temperatures and CO_2 data. The δ^{18}O curve is smoothed in order to clarify the gradual decrease over time. All data are available every 0.1 kyr. The thick lines represent 400-kyr running mean. Grey error bars indicate the standard deviation of model input and output. For CO_2 the error bar is calculated as 400-kyr running mean, for the other records it is the standard deviation on the 0.1 kyr value as used in the model. Data are available as a Supplement to this paper.

3 Results in terms of sea level and temperature trends

Our model-based deconvolution shows a long-term decrease in T_{NH} by 27 K since the Miocene (about 10 K in the global surface temperature) with superimposed orbitally forced changes (Fig. 1b). Eustatic sea level, more strictly sea level from ice-volume changes only, gradually falls, but is roughly constant from 13 Ma (+15 m) to 3 Ma (+5 m) as the ice sheets in the SH are full grown and major ice sheets in the NH are not yet developed (Fig. 1c). Moreover, the deviation of the sea level changes from the 400 kyr running mean revealed only low amplitude sea level changes of 10 m during this time period, whereas it fluctuated to $\pm$20 m prior to 13 Ma and up to $\pm$66 m after 3 Ma. Maximum sea level high-stand of +55 m occurred around 15 Ma, probably caused by a reduced EAIS (De Boer et al., 2010).

Figure 2 shows that there is not a unique solution for sea level given a certain temperature. This results from the different timescales in the coupled system of ice sheets, changing deep-water temperatures, surface temperatures, bedrock adjustment, and forcing and feedbacks of the mass balance height and albedo-temperature feedback. Obviously, sea level rises on average with temperature as illustrated by the thick lines in Fig. 2a. On average the sea level change is 6 m per Kelvin temperature change. Close to present-day

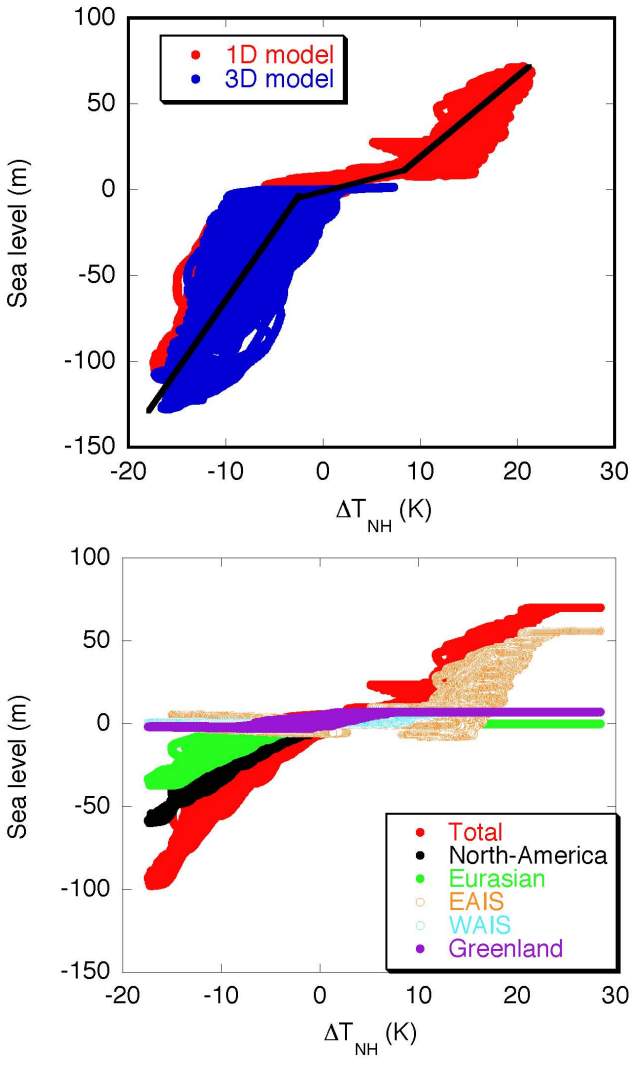

Fig. 2. **(a)** Sea level change is shown as a function of the reconstructed temperature for a set of 3-D NH ice sheets (blue) and for a set of five 1-D ice-sheet models (red) (Bintanja and Van de Wal, 2008; De Boer et al., 2010). The more sophisticated 3-D results are validated by observation of sea level (Lambeck and Chapell, 2001; Rohling et al., 2009). The 1-D results are in line for the colder climate condition with the 3-D results. The warm temperatures in combination with the sea level change resemble the melt of SH ice. The thick lines show the mean trends, emphasizing the low gradient for the present-day climate centred around zero. **(b)** The response of the individual ice sheets. Note the strong transient and nonlinear response for each ice sheet.

temperatures, i.e. $-2\,\mathrm{K} < \Delta T_{\mathrm{NH}} < +10\,\mathrm{K}$, only the GrIS and WAIS change in size. This results in only minor sea-level fluctuations, which are approximately 5 times lower compared to warm or cold conditions, expressed per Kelvin temperature change (Fig. 2b). During warmer ($\Delta T_{\mathrm{NH}} > +10\,\mathrm{K}$) and colder climates ($\Delta T_{\mathrm{NH}} < -2\,\mathrm{K}$), sea level changes are stronger due to variations in the size of the NAM, EAS and EAIS, for colder climates, NAIS, EAS and GrIS are vulnerable to changing temperature, whereas the WAIS and EAIS are sensitive to temperature changes during warmer climates. The sea level sensitivity to temperature change is approximately similar for warm ($6.5\,\mathrm{m\,K^{-1}}$) and cold ($7.8\,\mathrm{m\,K^{-1}}$) climates as indicated by the thick line in Fig. 2a. In addition, Fig. 2b shows the volume change for the individual ice sheets as a function of temperature leading by summation to the complex pattern in Fig. 2a. Also on the level of an individual ice sheet, transient effects impede a simple and unique solution between temperature and sea level, which implies that inverting climate information from sea level, has to be considered with great care.

In contrast to the sea level record, temperature shows a more gradual decline from the Miocene maximum around 15 Myr ago to the start of the major glaciation in the NH around 3 Ma. The gradual increase in the benthic δ^{18}O record leads to a long-term cooling of the climate between 13 and 3 Ma. The amplitude of temperature and sea level variability both increase once the major ice sheets develop in the NH around 3 Myr ago (Fig. 1).

Many tests have been performed with the model to assess the uncertainties in the input and model parameters on sea level and temperature results. The most important tests allow us to estimate the uncertainty range displayed in Fig. 1. For the δ^{18}O input we defined an uncertainty of 0.16 per mille, which is derived from the root-mean-squared difference between the smoothed marine record and the actual data points. The key model parameters contributing to the uncertainty are (1) the deep-water to surface-air temperature coefficient (range 0.15 to 0.25), (2) the temperature difference between T_{NH} and the temperatures around Antarctica (range: 6–14 K for EAIS, range: 2–10 K for WAIS), and (3) the isotopic content of the ice sheets (range from -43, -32, -28 to -55, -42, -36 per mille, respectively, for EAIS, WAIS, GrIS; see De Boer et al., 2010 for details). For the three model parameters, maximum and minimum values are used to test the effect on modelled temperature and sea level. The resulting standard deviation varies over time, but is on average 1.9 K for temperature and 6.2 m for sea level over the past 20 Myr. In order to interpret the results, one has to bear in mind that the reconstructed temperatures are strictly only valid in the continental areas of the NH where ice sheets develop (about 40°–80° N), implying that they are, therefore, not a representative for the entire globe (ΔT_{g}). A relationship between ΔT_{NH} and ΔT_{g} is developed later on.

4 Reconstruction of CO_2

In order to get a consistent CO_2 record, we investigated the relation between temperature and proxy CO_2 records based on B/Ca ratio (Tripati et al., 2009), stomata (Kürschner et al., 1996, 2008; Retallack 2009), δ^{11}B (Pearson and Palmer, 2000; Hönisch et al., 2009), alkenones (Pagani et al., 2005,

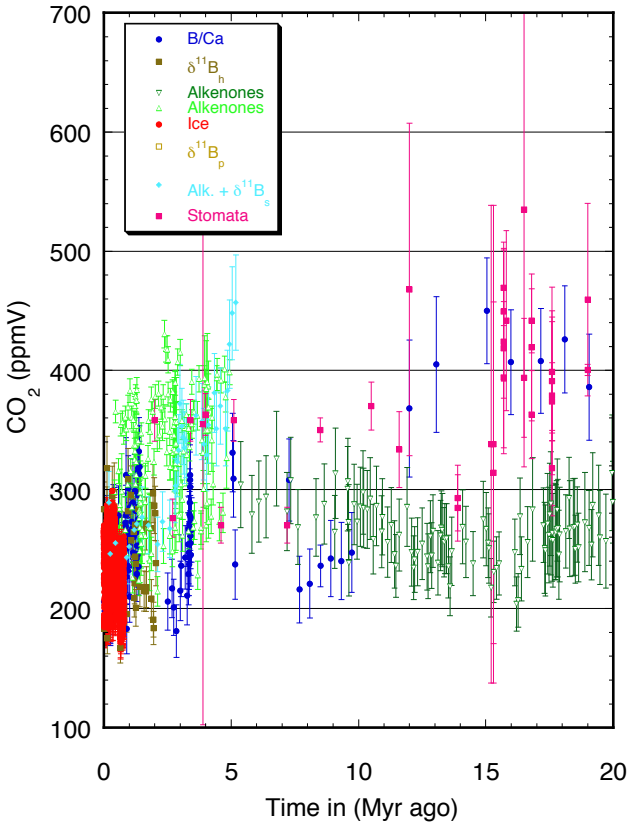

Fig. 3. CO_2 records as a function of time, indicating the inhomogeneous distribution in amount and range for the different proxies. Data are B/Ca (Tripati et al., 2009), stomata data (Kürschner et al., 1996, 2008; Retallack 2009), alkenones with $\delta^{11}B_s$ (Seki et al., 2010), $\delta^{11}B_p$ (Pearson and Palmer, 2000), $\delta^{11}B_h$ (Hönisch et al., 2009), alkenones (Pagani et al., 2005, 2010) and ice (Petit et al., 1999; Siegenthaler et al., 2005; Lüthi et al., 2008). The symbols and colours for the different proxies are similar in all figures. Alkenone data by Pagani et al. (2005, 2010) are treated as two datasets in order to test whether one of the two could be used for further analysis.

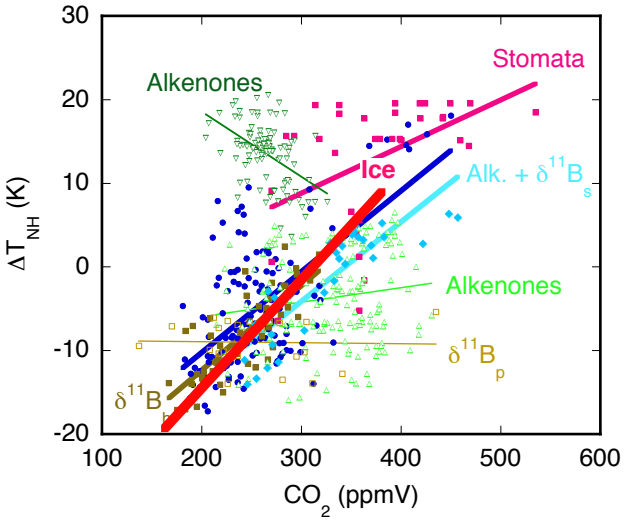

Fig. 4. Scatter plot of the different CO_2 proxies as a function of the reconstructed temperature, which is derived from the benthic $\delta^{18}O$ record as shown in Fig. 1. Only records with filled symbols $\delta^{11}B_h$ (Hönisch et al., 2009), B/Ca (Tripati et al., 2009), alkenones+ $\delta^{11}B_s$ (Seki et al., 2010), stomata data (Kürschner et al., 1996, 2008; Retallack 2009), and the ice-core record (Petit et al., 1999; Siegenthaler et al., 2005; Lüthi et al., 2008) are used for further analysis. For reasons of transparency CO_2 is plotted in ppmv. If CO_2 would be plotted as $\ln(CO_2/CO_{2,ref})$ a similar picture emerges. The latter is physically more consistent as it takes the saturation of the absorption bands into account.

2009), a combination of alkenones and $\delta^{11}B$ (Seki et al., 2010), and ice cores (Petit et al., 1999; Siegenthaler et al., 2005; Lüthi et al., 2008), all shown in Fig. 3. We did not consider the paleosol record presented by Beerling and Royer (2011) because of their large uncertainty. All data points are representative for different discrete time intervals, with obviously a bias towards the more modern data points and each having its advantages and drawbacks. For example, the boron isotope derived estimates of the CO_2 concentration are based on the fact that higher atmospheric concentrations lead to more dissolved CO_2 in the surface ocean, which causes a reduction in the pH of the ocean. As the pH can be derived from measurements of the $\delta^{11}B$ of calcium carbonate (Pearson and Palmer, 2000), CO_2 can be calculated provided that another parameter of the marine carbonate system (e.g. alkalinity) is known (Zeebe and Wolf-Gladrow, 2001). The method is expensive, time consuming and only well-preserved foraminiferal specimen are suitable for the analysis, resulting in only low-resolution records up to now. Ice cores provide the most robust and high-resolution CO_2 archive as they directly preserve the atmospheric concentrations, but only for the past 800 000 yr (Lüthi et al., 2008). Here, we accept all data as they are published without any further correction. The general picture is that the scatter in the different approaches is large, but there is a tendency for higher CO_2 values in the early Cenozoic (Ruddiman, 2003; Zachos et al., 2008), with ambiguous results for the last 20 Myr. Moreover, none of the proxies has a continuous record for the last 20 Myr (Fig. 3). For this reason there is a need to compile all available records in a consistent manner. The decomposition of the marine benthic $\delta^{18}O$ record offers a framework to do so.

We use the modelled temperature as a tool to select mutually consistent CO_2 records by assuming that there is a relation between CO_2 and ΔT_{NH}, which is comparable to the relation found in ice cores. In fact, this is justified as several independent proxies do show a similar linear relation (Fig. 4). Different methodologies may explain why the $\delta^{11}B_h$ ($\delta^{11}B$ from Hönisch et al., 2009) is more consistent with the ice cores CO_2 data then the $\delta^{11}B_p$ ($\delta^{11}B$ from Pearson and Palmer, 2000). Hönisch et al. (2009) selected samples

around glacial and interglacial extremes, which was not done by Pearson and Palmer (2000). In addition, it has been argued that the Pearson and Palmer (2000) data need to be rejected for reasons related to diagenesis, use of incorrect fractionation factors, and poor modelling of seawater alkalinity and $\delta^{11}B$ (Foster et al., 2006). The comparison in Fig. 4 reveals that the CO_2 estimates derived from the ice cores, B/Ca, stomata, $\delta^{11}B_h$ and the combination of alkenones and $\delta^{11}B_s$ ($\delta^{11}B$ from Seki et al., 2010) are mutually consistent, because they reveal similar slopes, whereas the $\delta^{11}B_p$, and alkenones-derived CO_2 estimates do not show a consistency with the ice-core record.

Hence, we selected only the consistent records to derive an empirical relationship between temperature and CO_2. This relation is used to calculate CO_2 from the reconstructed T_{NH} in order to generate a continuous CO_2 proxy series that is mutually consistent with the benthic $\delta^{18}O$ record. The application of the correlation between CO_2 and temperature implies, however, that the regression needs to cover the temperature range as shown in Fig. 1 without having too much bias to the data-rich cold climate state. For this reason, we binned the CO_2 observations in intervals of 1 K NH temperature change, for which results are shown in Fig. 5. The temperature records are running averages over 2000 yr, in order to prevent outliers due to a mismatch in dating of the CO_2 proxy and the benthic record. Furthermore, several tests have been performed to weigh the different accepted CO_2 proxies, by uncertainty in modelled temperature and measured CO_2. In addition, we tested the effect of the binning size and averaging period, which contribute to the uncertainty in the reconstructed CO_2. Omitting one of the proxies effects the end result by at most 6 % (B/Ca data) in the slope between $\ln(CO_2/CO_{2,ref})$. Based on all these tests, we eventually estimated an uncertainty of 10 % in the slope between $\ln(CO_2/CO_{2,ref})$ and ΔT_{NH} around a central value of 39 K. A log-linear regression between ΔT_{NH} and CO_2 is used because of the saturation of the absorption bands for CO_2 (Myhre et al., 1998). Accordingly, the CO_2 record as presented in Fig. 1 has an uncertainty of 20 ppmv for cold climates and up to 45 ppmv for warm climates. The larger uncertainty for warmer climates is due to the logarithmic relation between CO_2 and temperature.

Over the past 800 kyr the reconstructed CO_2 record is in good agreement with the ice-core record, (Fig. 6c), which is, however, input to the reconstruction and, therefore, not an independent result. Over the mid-Pleistocene transition (defined here from 1.5 to 0.5 Myr), our results indicate a gradual decline of about 23 ppmv, and at the same time an increase in the amplitude. Carbon-cycle simulation results over the last 2 Myr across the Mid-Pleistocene Transition (Köhler and Bintanja, 2008) support the change in amplitude, but suggest stable glacial CO_2 values and reduced interglacial CO_2. It is also unclear why the combined $\delta^{11}B$ and Alkenone record is higher than our reconstruction for the last 1.5 Myr.

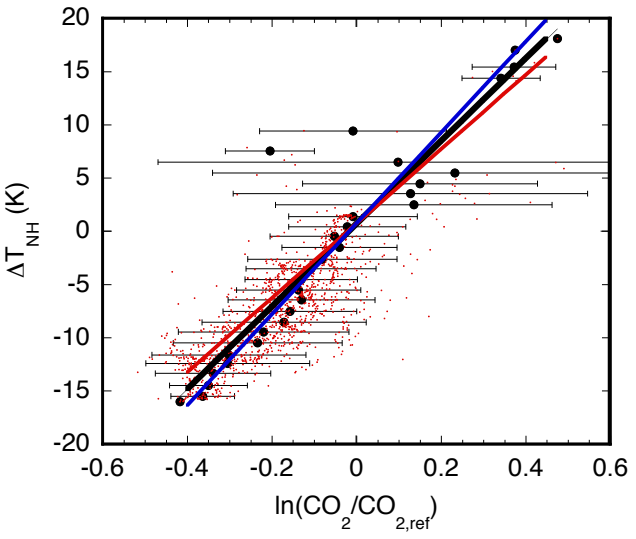

Fig. 5. The selected ($n = 1302$) proxy CO_2 data (red dots) binned in intervals of 1 K NH temperature change. The error bars represent one standard deviation variability of the data in the selected temperature interval. The additional lines show the range in C values from different weighing tests, blue C +10 %, red C −10 %. The slope of the regression line corresponding to C is 39 ± 3.9 K.

Around 10 Myr ago the B/Ca data measured on planktonic foraminifers indicate much lower CO_2 concentrations, in fact, more in line with the GEOCARB (carbon-cycle model, Berner, 1994) estimates (Fig. 6a). Ultimately this implies an inconsistency between benthic $\delta^{18}O$ reconstructions and B/Ca. The difference is too large to be attributed to model uncertainties.

5 Long-term knowledge on climate sensitivity

Since we now obtained a continuous record of T_{NH} and CO_2, we can address the long-term climate sensitivity in more detail. There are various ways to define climate sensitivity. Here we define climate sensitivity (S) as the functional dependency of changes in global surface temperature (ΔT_g) on CO_2, thus, $\Delta T_g = f(CO_2)$. It is calculated from the radiative forcing (ΔR) caused by changes in CO_2, other greenhouse gases, and various fast and slow feedbacks (f), which will be specified below. A general formulation for the global temperature is:

$$\Delta T_g = S\frac{\Delta R}{1-f} \quad (1)$$

In this general setting, changes in CO_2 might be the cause for climate change, thus, representing the forcing term ΔR or a feedback. A functional relationship between the global temperature and CO_2 can subsequently be developed, assuming that CO_2 is causing the radiative imbalance, $\Delta R = f(CO_2)$, while the initial perturbation of this imbalance might be

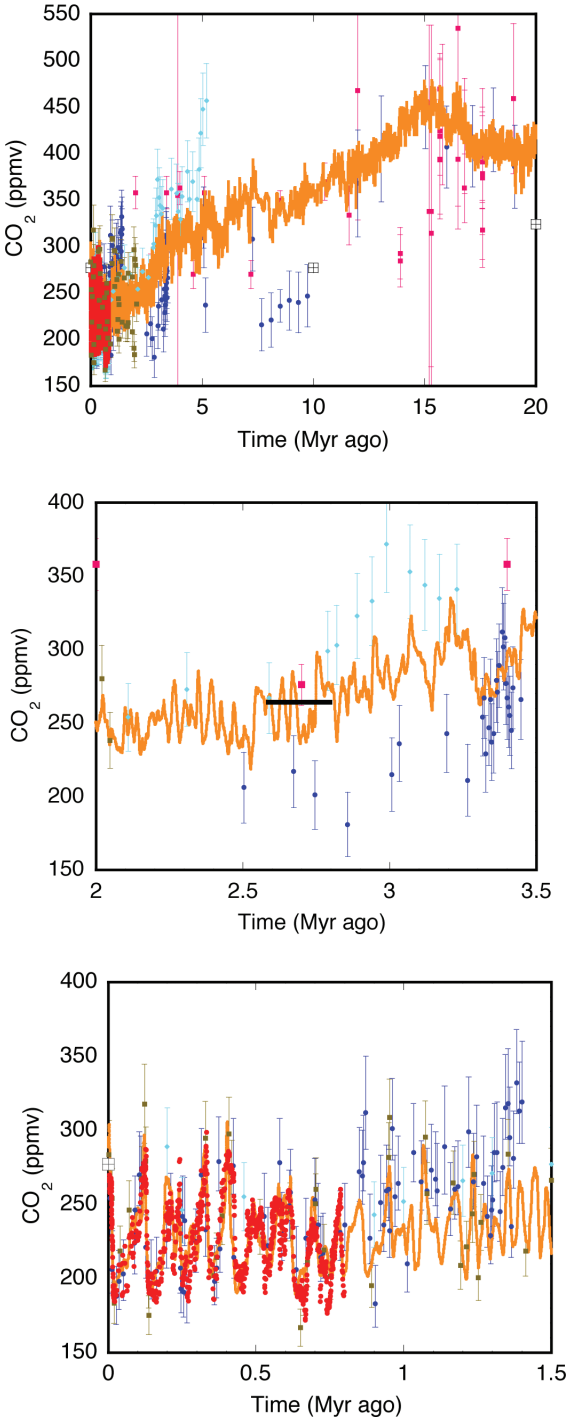

Fig. 6. Comparison of reconstructed CO_2 record with $C = 39$ K, with proxy records (symbols as in Fig. 3). Panel **(a)** for the full 20 Myr period, **(b)** for the period around the Northern Hemisphere glacial inception and **(c)** for the mid-Pleistocene transition. Note that the vertical scale is different for the different panels. The Horizontal bar in panel **(b)** indicates the onset of major glaciation in the Northern Hemisphere. The crosses with open squares are the GEOCARB data.

caused by other processes. This by no means implies that we believe that changes in CO_2 were always the driver for climate change over the last 20 Myr, but it is used to derive a functional relationship between ΔT_g and CO_2. The opposite procedure (forcing by other processes and feedbacks by CO_2) is certainly a valid option, but, for reasons of simplicity, here we follow only one of the two possible calculations.

From radiative transfer theory, we know that due to the saturation of the absorption bands, a logarithmic relationship has to be applied for the radiative forcing of CO_2:

$$\Delta R = \beta \ln \frac{CO_2}{CO_{2,ref}} \tag{2}$$

where ΔR is the radiative forcing in W m^{-2} and β is estimated to be 5.35 W m^{-2} (Myhre et al., 1998). This implies a radiative forcing of -2.4 W m^{-2} for the observed changes in CO_2 from LGM to present day, and +3.7 W m^{-2} for a doubling of CO_2, with $CO_{2,ref} = 278$ ppmv, the pre-industrial level. Non-CO_2 greenhouse gases like CH_4 and N_2O enhance this direct radiative forcing of CO_2. Hence, for the last 800 kyr this enhancement was about 30 % (Köhler et al., 2010), which is represented by $\gamma = 1.3$.

The sensitivity S of the climate system to external forcing is typically described by the Charney sensitivity S_c (Charney et al., 1979), which includes the fast feedbacks of the system (water vapour, lapse rate, albedo, snow and sea ice, clouds). It is the quantity usually calculated by coupled ocean-atmosphere models. Here, we use a sensitivity S_p derived from paleo data of 0.72 K/(W/m^2) (Köhler et al., 2010). It is based on a LGM cooling of $\Delta T_{g,LGM} = -5.8$ K (Schneider von Deimling et al., 2006) and a total radiative forcing $\Delta R_{LGM} = -9.5$ W m^{-2} (Köhler et al., 2010).

The total forcing of the system ($\Delta R'$) includes the forcing ΔR caused by all greenhouse gases, which is amplified by a feedback factor f consisting of the slow feedbacks not included in S_p. It represents the feedbacks from albedo changes caused by land ice, vegetation and dust.

$$\Delta R' = \frac{\gamma \Delta R}{1 - f} \tag{3}$$

For the last 800 kyr, a value for $f = 0.71$ and $\gamma = 1.3$ is derived from proxy-based evidence (Köhler et al., 2010). For ΔT_{NH} we obtain a value of -15.8 K averaged over the period 23 to 19 kyr BP (LGM), which is 2.7 times larger than the global temperature change of -5.8 K. This is in line with estimates of the polar amplification factor (α) from a GCM model of 2.5–3 by Singarayer and Valdes (2010). The final expression for the change of ΔT_{NH} can now be written as:

$$\Delta T_{NH} = C \ln \frac{CO_2}{CO_{2,ref}} \tag{4}$$

with

$$C = \frac{\alpha \beta \gamma S_p}{1 - f} \tag{5}$$

Calculation of C ($\alpha = 2.7$, $\beta = 5.35$, $\gamma = 1.3$, $S_p = 0.72$, $f = 0.71$, $CO_{2,ref} = 278$) results in an indicative value of 47.0 K for cold conditions (i.e. past 800 000 yr) as f is based on LGM proxy data. Where it might be noted that application of $CO_{2,ref} = 278$ ppmv implies that ΔT_{NH} is expressed relative to pre-industrial levels. This calculated value for C is, however, considerably larger than the 39 ± 3.9 K we found for the slope between $\ln(CO_2/CO_{2,ref})$ and ΔT_{NH} over the past 20 Myr (Fig. 5). Remarkably, Fig. 5 does not indicate that C depends on the CO_2 concentration itself. One might expect f to be smaller for warmer conditions, but this is apparently compensated by a change in one of the other parameters. From Fig. 5, it is clear that the scatter for warmer conditions is large and we have to await more proxy data for warmer conditions to see whether this log-linear relation holds.

A source of uncertainty is the value for S_p, which is derived from LGM conditions. Hargreaves et al. (2007) argued that this value is 15 % smaller than the value for $2 \times CO_2$, close to our derived values for the early Miocene climatic optimum. A similar change in the sensitivity implies that C would decrease to a value of 40.0 K, which is well within the uncertainty of our estimated value for C of 39 ± 3.9 K (Fig. 5).

Another source of uncertainty in this analysis is probably the assumption that the polar amplification factor, α, is constant over time. Theories and observations on much warmer climate states suggest a decrease in the meridional temperature gradient (e.g. Huber and Cabellero, 2011) implying a decrease in α. The fact that C does not vary with increased temperature suggests that a possible change in α or the long-term feedbacks compensate one another. The applied method does not allow separating α from the long-term feedbacks or the GHG forcing. In theory, if α were much smaller for warmer climate conditions and f smaller, it would imply that considerably higher CO_2 concentrations in the past are necessary to explain the temperatures derived from the benthic $\delta^{18}O$ record. However, the stomata-derived CO_2 data, the GeoCarb data (Berner 1994), and the B/Ca data do not indicate much higher CO_2 concentrations, at least not over the period considered here, suggesting that this theoretical example is not likely.

Too little information is available to attribute individual changes in the parameters over 20 Myr. But given the fact that the fitted value of C based on the presented data in this paper, and the estimated value of C based on our knowledge of the system (Köhler et al., 2010) are close to each other, implies that the combined effect of the key processes affecting benthic $\delta^{18}O$ records, temperature and CO_2 are incorporated sufficiently accurately for at least the period that there is ice on Earth. The implication of Eqs. (4) and (5) is that systematic errors in the various components can cancel each other very easily, complicating the interpretation of the sensitivity. A 20 % increase in α can be compensated by a 20 % decrease in β, γ, S_c or equally large increase of $(1 - f)$. As we determine C directly from the model inversion, one cannot expect improved insights in the different values for α, β, γ, S_c or f from our methodology. The fact that the values used in the literature eventually lead to a similar value for C merely indicates that there is no reason to adjust literature values for climate sensitivity based on the inversion used here.

To set our approach into context with existing calculations of climate sensitivity one might simply calculate the pure Charney climate sensitivity out of Eqs. (1), (4) and (5) by choosing $f = 0$ (no slow feedbacks of ice sheets and vegetation) and $\gamma = 1$ (no non-CO_2 GHG), which leads to $C = 7.2$ K and $\Delta T_g = 2.7$ K for a CO_2 doubling. This is close to the original value and well within the uncertainties of 3 ± 1.5 K (Charney et al., 1979).

For the interpretation of the climate sensitivity values one needs to be careful. In order to calculate temperature changes from CO_2 changes as presented in the literature often different feedbacks are included. Here, we use the feedback factor obtained by Köhler et al. (2010) based on paleo proxy evidence for the LGM to show that the value of C as obtained from our analysis are in agreement with estimates of α, β, γ and S_p and the 15 % reduction in S_p depending on the climate state as proposed by Hargreaves et al. (2007). Adopting a lower value for f as maybe deduced from Hansen et al. (2008) would indicate that our value for C would be too large. Of course this can be compensated by assuming a larger value for α, implying an even larger meridional temperature gradient, but that seems unlikely. In other words, the temperatures as we find them, based on the benthic records, support the feedback factor as derived by Köhler et al. (2010). If we extract this value ($f = 0.71$) from C to consider the short-term climate sensitivity and facilitate a more realistic comparison with Hansen et al. (2008), we yield a value for the sensitivity, which is smaller than the sensitivity by Hansen et al. (2008). Furthermore, Hansen et al. (2008) uses in their calculations a global LGM cooling of $\Delta T_g = -5$ K, while we refer to the temperature anomaly of -5.8 K, which is our understanding best supported by proxy data. This readily explains a similar larger difference of 16 % in the projected temperature changes of the two approaches calculated for future climate with doubled CO_2.

6 Discussion and conclusion

Accepting the CO_2 concentration as presented in Fig. 1 with all its caveats and limitations, completes the picture of the key climate variables over the last 20 Myr. The figure shows a gradual decline from about 450 ppmv around 15 Myr ago to a mean level during the last 1 Myr of 225 ppmv or a decrease of 225 ppmv. This is about 2.2 times the increase in CO_2 concentration over the last century as well as 2.2 times the range in the ice-core record over the past 800 kyrs. If we would have used only the ice-core record, we would have obtained

Middle Miocene values 300 ppmv above present-day level and the sensitivity would not agree with the analyses presented in the previous paragraph as the sensitivity (C) would decrease to a value as low as 28.5 K. Hence, the application of the inverse model and the stacked binning procedure is crucial for the results.

It should be realised that the results are as good as the input is for the model. We use the widely used benthic record by Zachos et al. (2008), which has δ^{18}O values during the Middle Miocene, which are comparable to their values at the E-O transition. As a consequence, our Middle Miocene ice volume is small. A test with the stacked record by Cramer et al. (2009), which addresses in more detail interbasin changes of δ^{18}O records, indicate a larger ice volume for the Middle Miocene. As a consequence temperature and CO_2 changes are differently, yielding Middle Miocene CO_2 values of 410 ppm.

The question remains of course what causes these subtle changes in the carbon cycle on the long timescale. In order to answer this question, much higher resolution and accuracy of CO_2 records are necessary. The large sensitivity implies that, in contrast to earlier conclusions (Hönisch et al., 2009), subtle changes in CO_2 (possibly internal), may have caused the MPT, when dominant 41-kyr glacial cycles evolved into a dominant 100-kyr rhythm (Van de Wal and Bintanja, 2009). Our results indicate an average change of only 23 ppmv between 1.5 Ma and 0.5 Ma, and also an increasing amplitude. This result seems to be more in line with a recent estimate by Lisiecki (2010) based on marine δ^{13}C measurements and the δ^{11}B data by Hönisch et al. (2009) than with the B/Ca derived CO_2 data by Tripati (2009), which indicates a larger change in CO_2 over the MPT. However, the trend in CO_2 over time is too small given the accuracy of the applied methods to draw firm conclusions on this point.

With respect to the inception of the Northern Hemisphere ice around 2.7 Myr ago, our results indicate that the trend in CO_2 before the inception is higher than the average rate of change (see Fig. 1d), and that the inception takes place once the long-term average concentration drops below 265 ± 20 ppmv (Fig. 6b). So for this climate transition a change in CO_2 seems to be more important than for the mid-Pleistocene transition.

In conclusion, the self-consistency of our approach should enable researchers from various disciplines to identify more easily whether new CO_2 proxies are in line with the reconstructed temperature change derived from the δ^{18}O record and the ice core derived CO_2, $\delta^{11}B_h$, $\delta^{11}B_s$ + alkenones, B/Ca and stomata. It is tempting to use the newly reconstructed CO_2 to address the long-term climate sensitivity, but the approach is not accurate enough to revise current ideas about climate sensitivity because no clear distinction can be made between the various feedbacks and possibilities for compensating mechanisms. Various geological processes important during the last 20 Myr such as mountain uplift (e.g. Foster et al., 2010) and changes in the gateways are not considered here. However, for global climate changes, CO_2 induced changes dominate, as shown by Henrot et al. (2010) who based their argument on a model of intermediate complexity that geological processes like mountain building and changes in ocean gateways, are of secondary importance for global temperature and can not explain the proxy reconstructions of the change in temperature within their modelling framework. Based on the analyses of climate sensitivity, we argue that the applied method, in combination with the available data, is not accurate enough to revise ideas on climate sensitivity. Compensating effects prevent the unravelling of the different contributions to the log-linear relation between CO_2 and temperature.

As a final remark, we stress that the relation between CO_2 and the Northern Hemisphere temperature may change, for instance, by a changing strength of feedbacks or a different relation between global and Northern Hemisphere temperature changes, and as such it complicates the interpretation of paleo data as analogue for present day conditions. Paleo data provide the range of natural fluctuations, but the rate of change of key variables is shown to be depending on the state of the system (Köhler et al., 2010), the timescale of interest and the processes at stake, which are not necessarily similar in the past as for present day climate change. Paleo data should be interpreted in the context of the conditions and forcing prevailing at that time.

Supplementary material related to this article is available online at: http://www.clim-past.net/7/1459/2011/ cp-7-1459-2011-supplement.zip.

Acknowledgements. Financial support to B. de Boer was provided by the Netherlands Organization of Scientific Research (NWO) in the framework of the Netherlands Polar Programme. P. Köhler is funded by PACES, the research program of AWI.

Edited by: V. Rath

References

Barker, S., Diz, P., Vantravers, M. J., Pike, J., Knorr, G., Hall, I. R., and Broecker, W. S.: Interhemispheric Atlantic seesaw response during the last deglaciation, Nature, 457, 1007–1102, 2010.

Beerling, D. J. and Royer, D. L.: Convergent Cenozoic CO_2 history, Nat. Geosci., 4, 418–420, doi:10.1038/ngeo1186, 2011.

Berner, R. A., GEOCARB II: A revised model of atmospheric CO_2 over Phanerozoic time, Am. J. Sci., 294, 56–91, 1994.

Bintanja, R. and Oerlemans, J.: The effect of reduced ocean overturning on the climate of the last glacial maximum, Clim. Dynam., 12, 523–533, 1996.

Bintanja, R. and van de Wal, R. S. W.: North American ice-sheet dynamics and the onset of 100,000-year glacial cycles, Nature, 454, 869–872, 2008.

Bintanja, R., van de Wal, R. S. W., and Oerlemans, J.: A new method to estimate ice age temperatures, Clim. Dynam., 24, 197–211, 2005a.

Bintanja, R., van de Wal, R. S. W., and Oerlemans, J.: Modelled atmospheric temperatures and global sea levels over the past million years, Nature, 437, 125–128, doi:10.1038/nature03975, 2005b.

Charney, J. G., Arakawa, A., Baker, D. J., Bolin, B., Dickinson, R. E., Goody, R. M., Leith, C. E., Stommel, H. M., and Wunsch, C. I.: Carbon Dioxide and Climate: A Scientific Assessment, National Academy of Science, 33 pp., 1979.

Clark, P. U., Alley, R. B., and Pollard, D.: The middle Pleistocene transition : Characteristics, mechanisms, and implication for long-term changes in atmospheric pCO_2. Quat. Sci. Rev., 25, 3150–3184, 2006.

Cramer, B. S., Toggweiler, J. R., Wright, J. D., Katz, M. E., and Miller, K. G.: Overturning since the Late Cretaceous: inferences from a new benthic foraminferal isotope compilation, Paleoceanography, 24, PA4216, doi:10.1029/2008PA001683, 2009.

De Boer, B., van de Wal, R. S. W., Bintanja, R., Lourens, L. J., and Tuenter, E.: Cenozoic global ice-volume and temperature simulations with 1-D ice-sheet models forced by benthic δ^{18}O records, Ann. Glaciol., 51, 23–33, 2010.

De Boer, B., van de Wal, R. S. W., Lourens, L. J., and Bintanjav, R.: Transient nature of the Earth 's climate over the past 35 Million year, Paleogeogr. Paleoclim., in press, doi:10.1016/j.paleo.2011.02.001, 2011.

Duplessy, J.-C., Labeyrie, L., and Waelbroeck, C.: Constraints on the oxygen isotopic enrichment between the Last Glacial Maximum and the Holocene: paleoceanographic implications, Quat. Sci. Rev., 21, 315–330, 2002.

Foster, G. L., Ni, Y., Haley, B., and Elliott, T.: Accurate and precise isotopic measurement of sub-nanogram sized samples of foraminiferal hosted boron by total evaporation NTIMS, Chem. Geol., 230, 161–174, 2006.

Foster, G. L., Lunt, D. J., and Parrish, R. R.: Mountain uplift and the glaciation of North America – a sensitivity study, Clim. Past, 6, 707–717, doi:10.5194/cp-6-707-2010, 2010.

Hansen, J., Sato, M., Kharecha, P., Beerling, D., Berner, R., Masson-Delmotte, V., Pagani, M., Raymo, M., Royer, D. L., and Zachos, J. C.: Target atmospheric CO_2: where should humanity aim?, Open Atmos. Sci. J., 2, 217–231, 2008.

Hargreaves, J. C., Abe-Ouchi, A., and Annan, J. D.: Linking glacial and future climates through an ensemble of GCM simulations, Clim. Past, 3, 77–87, doi:10.5194/cp-3-77-2007, 2007.

Hays, J. D., Imbrie, J., and Shackleton, N. J.: Variations in the Earth's orbit: Pacemaker of the ice ages, Science, 194, 1121–1132, 1976.

Henrot, A.-J., François, L., Favre, E., Butzin, M., Ouberdous, M., and Munhoven, G.: Effects of CO_2, continental distribution, topography and vegetation changes on the climate at the Middle Miocene: a model study, Clim. Past, 6, 675–694, doi:10.5194/cp-6-675-2010, 2010.

Hönisch, B., Hemming, N. G., Archer, D., Siddall, M., and McManus J. F.: Atmospheric carbon dioxide concentration across the mid-Pleistocene transition, Science, 324, 1551–1553, 2009.

Huber, M. and Caballero, R.: The early Eocene equable climate problem revisited, Clim. Past, 7, 603–633, doi:10.5194/cp-7-603-2011, 2011.

Huybers, P.: Glacial variability over the last two million years: An extended depth-derived age model, continuous obliquity pacing, and the Pleistocene progression, Quat. Sci, Rev. 26, 37–55, 2007.

Imbrie, J. and Imbrie, J. Z.: Modelling the climatic response to orbital variations, Science, 207, 942–953, 1980.

Jansen, E. J., Overpeck, J., Briffa, K. R., Duplessey, J.-C., Joos, F., Masson-Delmotte, V., Olago, D., Otto-Bliesner, B., Peltier, W. R., Rahmstorf, S., Ramesh, R., Raynaud, D., Rind, D., Solomina, O., Villalba, R., and Zhang, D.: Paleoclimate, In Climate change 2007: The physical Science basis, Contribution of Working Group I to the Fourth Assessment Report of the Intergovernmental Panel on Climate Change, 433–497, 2007.

Köhler, P. and Bintanja, R.: The carbon cycle during the Mid Pleistocene Transition: the Southern Ocean Decoupling Hypothesis, Clim. Past, 4, 311–332, doi:10.5194/cp-4-311-2008, 2008.

Köhler, P., Bintanja, R., Fischer, H., Joos, F., Knutti, R., Lohmann, G., and Masson-Delmotte, V.: What caused Earth's temperature variations during the last 800,000 years?, Data-based evidence on radiative forcing and constraints on climate sensitivity, Quat. Sci. Rev., 29, 129–145, 2010.

Kürschner, W. M., van der Burgh, J., Visscher, H., and Dilcher, D. L.: Oak leaves as biosensors of late Neogene and early Pleistocene paleoatmospheric CO_2 concentrations, Marine Micropaleont., 27, 299–312, 1996.

Kürschner, W. M., Kvacek, Z., and Dilcher, D. L.: The impact of Miocene atmospheric carbon dioxide fluctuations on climate and the evolution of terrestrial ecosystems, Proc. Nat. Aca. Sci., 105, 449–453, 2008.

Lambeck, K. and Chapell, J.: Sea level change through the last glacial cycle, Science, 292, 679–686, 2001.

Lawrence, K. T., Zhonghui, L., and Herbert, T. D.: Evolution of the eastern tropical Pacific through Plio-Pleistocene glaciation, Science, 312, 79–83, 2006.

Lear, C. H., Elderfield, H., and Wilson, P. A.: Cenozoic deep-sea temperatures and global ice volumes from Mg/Ca in benthic foraminiferal calcite, Science, 287, 269–272, 2000.

Lear, C. H., Mawbey, E., and Rosenthal, Y.: Cenozoic benthic foraminiferal Mg/Ca and Li/Ca records: Toward unlocking temperatures and saturation states, Paleoceanography, 25, 1–11, doi:10.1029/2009PA001880, 2010.

Lisiecki, L. E.: A benthic δ^{13}C-based proxy for atmospheric PCO_2 over the last 1.5 Myr, Geophys. Res. Lett., 37, L21708, doi:10.1029/2010GL045109, 2010.

Lüthi, D., Floch, M. Le, Bereiter, B., Blunier, T., Barnola, J-M., Siegenthaler, U., Raynaud, D., Jouzel, J., Fischer, H., Kawamura K., and Stocker, T. F.: High-resolution carbon dioxide concentration record 650,000–800,000 years before present, Nature, 453, 379–382, 2008.

Milankovitch, M.: Kanon der Erdbestrahlung und seine Anwendung auf das Eiszeitenproblem, Special Publications, Royal Serbian Acadademy, 132, 1941.

Miller, K. G., Kominz, M. A., Browning, J. V., Wright, J. D., Mountain, G. S., Katz, M. E., Sugarman, P. J., Cramer, B. S., Christie-Blick, N., and Pekar, S. F.: The Phanerozoic record of global sea level change, Science, 310, 1293–1298, 2005.

Müller, R. D., Sdrolias, M., Gaine, C., Steinberger, B., and Heine, C.: Log-term sea-level fluctuations driven by ocean basin dynamics, Science, 319, 1357–1362, 2008.

Myhre, G., Highwood, E. J., Shine, K. P., and Stordal, F.: New es-

timates of radiative forcing due to well mixed greenhouse gases, Geophys. Res. Lett., 25, 2715–2718, 1998.

Pagani, M., Zachos, J. C., Freeman, K., Tipple, B., and Bohaty, S.: Marked decline in atmospheric carbon dioxide concentrations during the Paleogene, Science, 309, 600–603, 2005.

Pagani, M., Liu, Z., LaRiviere, J., and Ravelo, A.: High Earth-system climate snsitivity determined from Pliocene carbon dioxide concentrations, Nat. Geosci., 3, 27–30, 2009.

Pearson, P. N. and Palmer, M. R.: Atmospheric carbon dioxide concentrations over the past 60 million years, Nature, 406, 695–699, 2000.

Petit, J. R., Jouzel, J., Raynaud, D., Barkov, N. I., Barnola, J.-M., Basile, I., Bender, M., Chapellaz, J., Davis, M., Delaygue, G., Delmotte, M., Kotlyakov, V. M., Legrand, M., Lipenkov, V. Y., Lorius, C., Pépin, L., Ritz, C., Saltzmann, E., and Stievenard, M.: Climate and atmospheric history of the past 420000 years from the Vostok ice core, Antarctica, Nature, 399, 429–436, 1999.

Raymo, M. E: The initiation of Northern Hemisphere glaciation, Annu. Rev. Earth Planet. Sci., 22, 353–383, 1994.

Retallack, G. J.: Greenhouse crises of the past 300 million years, GSA Bulletin, 121, 1441–1455, 2009.

Rohling, E. J., Grant, K., Bolshaw, M., Roberts, A. P., Siddall, M., Hemleben, Ch., and Kucera, M.: Antarctic temperature and global sea level closely coupled over the past five glacial cycles, Nat. Geosci., 2, 500–504, 2009.

Ruddiman, W. F.: Earth's climate, W.H. Freeman and Company, 2001.

Ruddiman, W. F.: Orbital insolation, ice volume and greenhouse gases, Quat. Sci. Rev., 22, 1597–1629, 2003.

Ruddiman, W. F.: A paleoclimatic Enigma?, Science, 328, 838–839, doi:10.1126/science.1188292, 2010.

Schneider von Deimling, T., Ganopolski, A., Held, H., and Rahmstorf, S.: How cold was the Last Glacial Maximum?, Geophys. Res. Lett., 33, L14709, doi:10.1029/2006GL026484, 2006.

Seki, O., Foster, G. L., Schmidt, D. N., Mackensen, A., Kawamura, K., and Pancost, R. D.: Alkenone and boron-based Pliocene pCO_2 records, Earth Planet. Sci. Lett., 292, 201–211, 2010.

Shackleton, N. J.: Attainment of isotopic equilibrium between ocean water and the benthonic foraminifera genus Uvigerina: isotopic changes in the ocean during the last glacial, Cent. Nat. Sci. Colloq. Int., 219, 203–209, 1974.

Siegenthaler, U., Stocker, T. F., Monnin, E., Lüthi D., Schwander, J., Stauffer, B., Raynaud, D., Barnola, J., Fischer H., Masson-Delmotte, V., and Jouzel, J.: Stable carbon cycle-climate relationship during the Late Pleistocene, Science, 310, 1313–1317, 2005.

Singarayer, J. S. and Valdes, P. J.: High-latitude climate sensitivity to ice-sheet forcing over the last 120 kyr, Quat. Sci. Rev., 29, 43–55, 2010.

Tripati, A. K., Roberts, C. D., and Eagle, R. A.: Coupling of CO_2 and ice sheet stability over major climate transitions of the last 20 million years, Science, 326, 1394–1397, 2009.

Tziperman, E. and Gildor, H.: On the mid-Pleistocene to 100-kyr glacial cycles and the asymmetry between glaciation and deglaciation times, Paleooceanography 18, 1001, doi:10.1029/2001PA000627, 2003.

Van de Wal, R. S. W. and Bintanja, R.: Changes in temperature, ice and CO_2 during the Mid-Pleistocene Transition, Science, E Letter, 18 September 2009, 2009.

Zachos, J. C., Dickens, G. R., and Zeebe, R. E.: An early Cenozoic perspective on greenhouse warming and carbon-cycle dynamics, Nature, 451, 279–283, 2008.

Zeebe, R. E. and Wolf-Gladrow, D. A.: CO_2 in Seawater: Equilibrium, Kinetics, Isotopes. Elsevier Science Publishing, Elsevier Oceanography Book Series, 65, 346 pp., 2001.